ISSN 1070-4272, Russian Journal of Applied Chemistry, 2006, Vol. 79, No. 11, pp. 1902–1906. © Pleiades Publishing, Inc., 2006.
Original Russian Text © N.E. Kotel'nikova, E.L. Lysenko, R. Serimaa, K. Pirkkalainen, U. Vainio, A.L. Shakhmin, N.N. Saprykina, V.K. Lavrent'ev, D.A. Medvedeva, N.P. Novoselov, 2006, published in Zhurnal Prikladnoi Khimii, 2006, Vol. 79, No. 11, pp. 1924–1928.

MACROMOLECULAR CHEMISTRY AND POLYMERIC MATERIALS

Cellulose Matrix as a Nanoreactor for Preparing Nanoparticles of Nickel and Its Oxides Using Hydrazine Dihydrochloride as Reductant

N. E. Kotel'nikova, E. L. Lysenko, R. Serimaa, K. Pirkkalainen, U. Vainio, A. L. Shakhmin, N. N. Saprykina, V. K. Lavrent'ev, D. A. Medvedeva, and N. P. Novoselov

Institute of Macromolecular Compounds, Russian Academy of Sciences, St. Petersburg, Russia
State University of Technology and Design, St. Petersburg, Russia
University of Helsinki, Helsinki, Finland
Prikladnaya Khimiya Russian Scientific Center, Federal State Unitary Enterprise, St. Petersburg, Russia

Received May 24, 2006

Abstract—A matrix of microcrystalline cellulose was used as a nanoreactor for the reduction of Ni(II) ions with hydrazine dihydrochloride.

DOI: 10.1134/S1070427206110310

Numerous polymeric nanocomposites with preset physicochemical properties [1], containing stabilized metal (Ag, Cu, Ni, Pt, Pd, etc.) nanoparticles [2–7], have been prepared by now. Nanoparticles of some metals, e.g., Ni, impart fo polymeric nanocomposites magnetic and catalytic properties [8]; however, the preparation of Ni(0) nanoparticles is complicated because Ni metal is readily oxidized [9].

Recently the interest in preparation of metal nanoparticles in ordered solid matrices (nanoreactors) increased, because in these matrices, in contrast to polymer solutions, significant aggregation of nanoparticles can be avoided [1]. Among promising nanoreactors is cellulose, a natural polymer characterized by a highly porous system of conjugated fibers. It has a large specific surface area and is successfully used as a solid matrix for intercalation of transition metal (Ag, Pt, Pd, Cu) nanoparticles [10–12]. Papers on the intercalation of Ni nanoparticles into natural polymers (in particular, cellulose) are few [13, 14]. Ishiyama et al. [13] reported on the preparation of 5–21-nm particles of Ni and its oxide in a gel membrane of cellulose acetate by thermal decomposition of the membrane after the intercalation of Ni^{2+} ions.

This paper continues our studies of the use of a cellulose matrix as a nanoreactor for intercalation of nanoparticles of zero-valent metals (in particular, Ni) and their oxides [15]. Nanocomposites based on cellulose and nickel can be used in catalysis and also as magnetic and conducting materials.

EXPERIMENTAL

Cellulose samples containing nanoparticles of Ni(0) or its oxides were prepared by diffusion of Ni^{2+} ions into a cellulose matrix from a solution of nickel nitrate $Ni(NO_3)_2 \cdot 6H_2O$, followed by reduction of Ni^{2+}. As a matrix we used microcrystalline cellulose (MCC) prepared by acid hydrolysis according to [10]; it was a powder with the particle size less than 0.06 mm and moisture content not exceeding 1 wt %. As a reductant for Ni^{2+} we used hydrazine dihydrochloride $N_2H_4 \cdot 2HCl$ (Reaktiv Joint-Stock Company, St. Petersburg). It is known that nickel ions are reduced with $N_2H_4 \cdot 2HCl$ only in alkaline solutions containing complexing anions at a large excess of the reductant and elevated temperatures [16].

A 1-g sample of MCC was vigorously stirred with 20 ml of a 0.05 or 0.1 M citrate solution of nickel nitrate for 1 h; the diffusion temperature was varied from 20 to 95°C. The $C_m(C_6H_5O_7^{3-})/C_m(Ni^{2+})$ ratio was 1 : 1. Citrate ions served as ligands for Ni^{2+} ions, preventing the precipitation of nickel hydroxide in a strongly alkaline medium; also, being sorbed on the forming metal particles and imparting to them a negative charge, they prevented the particle aggregation.

Nickel content in the bulk and on the surface of MCC-Ni samples and crystallite size of Ni and MCC

Sample no.	Temperature of Ni^{2+} diffusion, °C	Ni content, wt %		Crystallite size (XPA), nm	
		in the bulk (elemental analysis)	on the surface (XPES)	MCC	Ni(0)
1	20	6.9	31.5	7.5 ± 0.3	10.8 ± 1.0
2	70	7.4	17.4	7.5 ± 0.3	12.3 ± 1.0
3	95	10.0	18.7	7.4 ± 0.3	13.5 ± 1.0

To a suspension obtained after the diffusion of Ni^{2+}, we added with vigorous stirring a solution prepared by dissolving a weighed portion of $N_2H_4 \cdot 2HCl$ in 20 ml of 3 M NaOH. The $N_2H_4 \cdot 2HCl$ concentration in this solution was varied from 0.5 to 4 M, so that the molar ratio $C_m(N_2H_4 \cdot 2HCl)/(C_m(Ni^{2+})$ (MR) was varied from 5 to 40. The reduction was performed at 95°C for 0.5–2 h.

After the reduction, the precipitate was separated on a glass frit and washed with water and ethanol. The washing completeness was judged from the neutral reaction of the wash waters and negative reaction for the Ni^{2+} ions with dimethylglyoxime [17]. The samples after vacuum drying at 40°C were powders of the color varying from light green to black. All the chemicals used in the synthesis were of pure or analytically pure grade. The nickel-containing cellulose materials obtained by this procedure are hereinafter designated as MCC-Ni.

The nickel concentration in the bulk of MCC-Ni samples was determined by elemental analysis, and that on the sample surface, by X-ray photoelectron spectroscopy (XPES). The oxidation state of Ni on the fiber surface was also determined by XPES. The sample structure, nickel oxidation state in the bulk of cellulose, and changes in the chemical composition were studied by X-ray phase analysis (wide-angle X-ray scattering, XPA) and IR Fourier spectroscopy. The procedures for sample preparation and calculations are described elsewhere [10]. The morphology of MCC-Ni samples and the nickel particle size and particle-size distribution were studied by scanning electron microscopy (SEM) [15].

The experimental conditions strongly affect both the amount of Ni intercalated into the MCC matrix and its oxidation state in MCC-Ni samples. For example, as the temperature of Ni^{2+} diffusion into the MCC matrix in the first step of the process was increased from 20 to 95°C, the amount of the intercalated nickel after the subsequent reduction appreciably increased (from 6.9 to 10.0 wt %) at any $C_m(N_2H_4 \cdot 2HCl)/C_m(Ni^{2+})$. A similar trend was observed when $NaBH_4$ and KH_2PO_2 were used as reductants [15].

Another factor strongly affecting the Ni content in the final products is the reductant concentration. As the MR was increased from 5 to 40, the Ni content in the bulk of MCC increased until the maximal value of 10.0 wt % was attained. An increase in the reductant concentration also favors the reduction of Ni^{2+} to Ni(0). It is known that the color of the samples obtained characterizes the oxidation state of Ni in the samples [18]. An increase in the MR from 5 to 40 led to a change in the sample color from light green or greenish-brown, caused by the presence of $Ni(OH)_2$, to light gray (at MR = 15) and then dark gray (at MR = 20 and over), characteristic of finely dispersed Ni(0). Thus, the reduction of Ni^{2+} to Ni(0) is possible only at a high concentration of the reductant, hydrazine dihydrochloride (MR $\geq$ 15–40). The maximal amount of nickel introduced into the cellulose matrix (10.0 wt %) corresponds to 0.289 mol of Ni per mole of MCC units. With $NaBH_4$ and KH_2PO_2 used as reductants, the maximal Ni content (molar ratio to MCC units) was 0.315 and 0.358 (11.1 and 12.8 wt %), respectively [15]. All these values are close, i.e.,

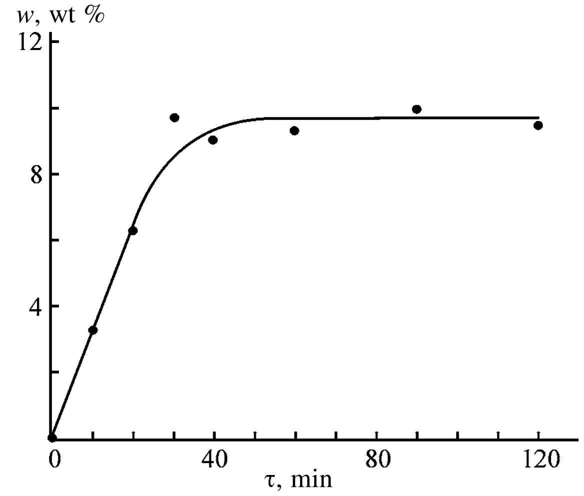

Fig. 1. Kinetic curve of Ni^{2+} reduction with $N_2H_4 \cdot 2HCl$. $C_m(Ni^{2+})$ 0.1 M, MR = 30, diffusion and reduction temperature 95°C. (*w*) Ni content and (τ) time.

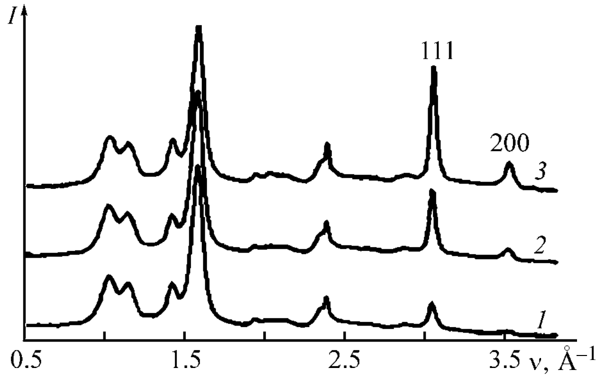

Fig. 2. Diffraction patterns of MCC-Ni sample nos. 1–3 prepared at MR = 30; reduction temperature 95°C. (*I*) X-ray scattering intensity and (ν) scattering angle. (*1–3*) Sample nos. 1–3 (see table), respectively; the same for Fig. 3.

about 1 mol of Ni was intercalated per 3 cellulose units with all the three reductants.

One of the major factors affecting the nickel content in the final products is the reduction time. The dependence of the nickel content in MCC-Ni samples on the reduction time (Fig. 1) shows that the equilibrium content of Ni in the MCC matrix is attained in 0.5 h and does not further change in the subsequent 1.5 h. The apparent rate constant of the pseudo-first-order reaction under these experimental conditions (the reaction was performed at MR = 30), calculated from the semilog plot, was $k = 2.7 \times 10^{-2}$ min^{-1}. The lower the MR, the slower the reduction. At MR = 20, the reaction rate decreases by a factor of approximately 3. It should be noted that the rate of the Ni^{2+} reduction with $N_2H_4 \cdot 2HCl$ exceeded by an order of magnitude the rate of its reduction with KH_2PO_2 reported in [15].

As shown above, an increase in the reductant concentration leads to a proportional increase in the Ni content in the bulk and to the reduction of Ni^{2+} to Ni(0). This was confirmed by XPA. The scattering curves of samples prepared at MR = 20 contained strong reflections of nickel oxide in the region of 2θ 36.8° and 42.9° and weak reflections of Ni(0) in the region of 2θ 44.3° and 51.2° ([111] and [200], respectively). With an increase in the MR to 30, the X-ray scattering curves of MCC-Ni samples differing only in the temperature of diffusion of Ni^{2+} into the MCC matrix (Fig. 2) contained Ni(0) reflections, and their intensity was proportional to the nickel content in the sample. This fact indicates that Ni(0) was the major nickel form in the bulk of these samples. The mean size of the crystallites, determined from the [111] reflections, was 10.8–13.5 nm (see table). Thus, XPA

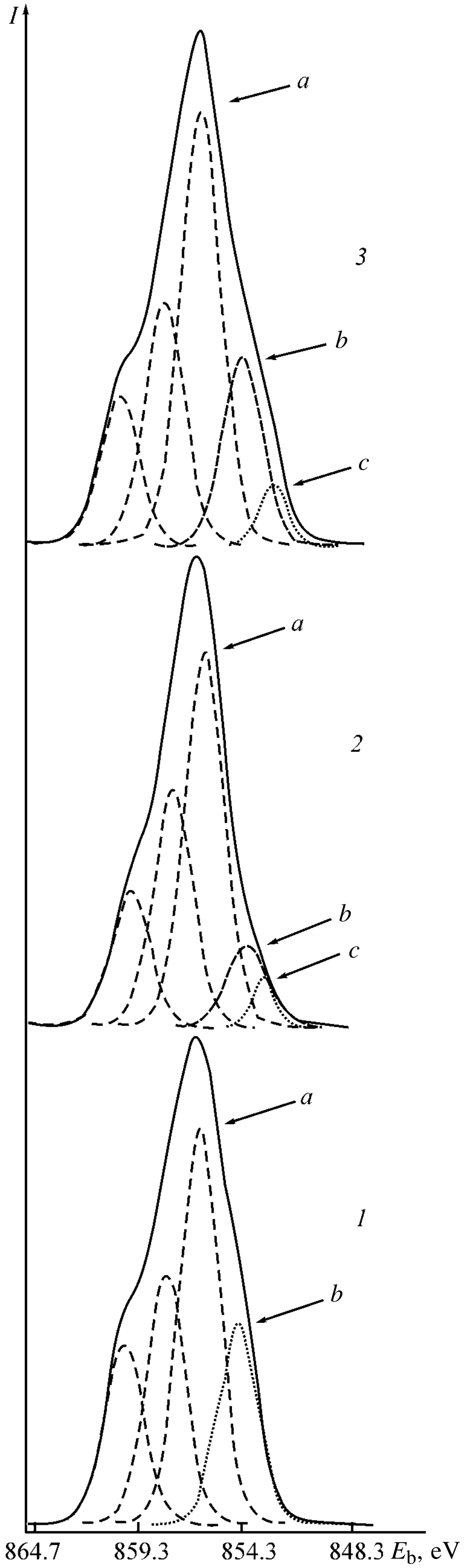

Fig. 3. XPE spectra of MCC-Ni sample nos. 1–3: (*I*) Intensity and (E_b) binding energy.

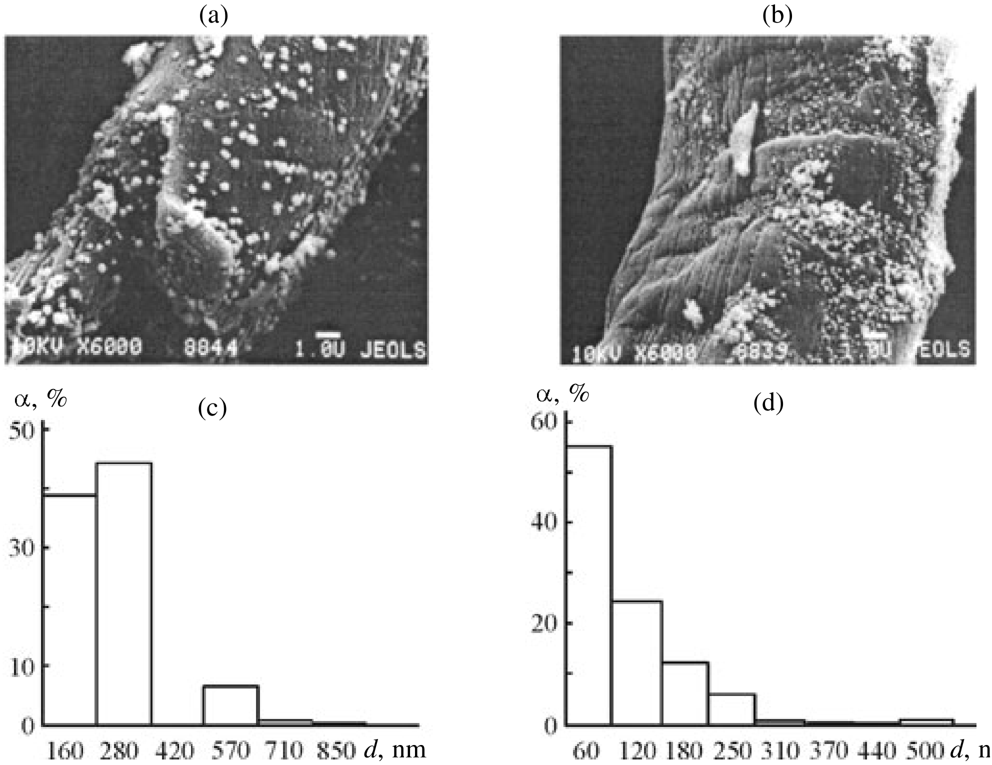

Fig. 4. Electron micrographs of MCC-Ni sample nos. (a) 1 and (b) 2; histograms of the distribution of Ni nanoparticles on the surface of sample nos. (c) 1 and (d) 2 with respect to the particle diameter. (α) Fraction of particles and (*d*) particle diameter.

confirmed the presence of the nanodispersed crystalline phase of Ni(0) in the bulk of the samples.

As in the case of reduction of Ni^{2+} with $NaBH_4$ and KH_2PO_2, the formation of nickel nanoparticles in the cellulose matrix did not affect the MCC crystal structure. The structural morphology of cellulose I, characteristic of MCC, was preserved, and the size (width) of MCC crystallites in MCC-Ni samples was close to that in the initial MCC (7.4 ± 0.1 nm, see table).

Thus, by intercalation of nickel in an MCC matrix we prepared MCC-Ni nanocomposites containing in the bulk mainly Ni(0) nanoparticles; the Ni oxidation state and crystallite size depended on the experimental conditions and primarily on the reductant concentration.

A comparison of the IR Fourier spectra of the MCC-Ni (at the maximal Ni content in the bulk) samples with that of the initial MCC revealed a minor decrease in the intensity of the absorption band at 3000–3600 cm^{-1} belonging to the stretching virbations of OH groups participating in inter- and intramolecular hydrogen bonds. Apparently, intercalation of Ni into a cellulose matrix is accompanied by cleavage of a small amount of hydrogen bonds on the surface of cellulose fibrils, followed by their redistribution.

The nickel concentration on the surface of fibers, determined by XPES, exceeds by a factor of 1.8–4.6 the nickel content in the bulk (see table). The ratio of redox forms on nickel on the surface is also different. Figure 3 shows the XPE spectra of the Ni $2p_{3/2}$ line and the resolution of spectral lines into four or five major components in MCC-Ni sample nos. 1–3. The components correspond to the Ni $2p_{3/2}$ binding energy in Ni_2O_3 (E_b = 856.7 eV, components *a*), NiO (E_b = 854.8 eV, components *b*), and Ni(0) (E_b = 853.4 eV, components *c*) [19]. The Ni(0) content on the fiber surface in sample nos. 2 and 3 (2.8 and 4.1 wt %, respectively) is considerably lower than that of nickel oxides. The high content of nickel oxides on the sample surface is due to the high susceptibility of Ni(0) nanoparticles to oxidation with atmospheric oxygen [9]. Thus, the samples obtained are not uniform in the chemical composition of nickel on the surface. It should be noted that the spectra of all the samples have also components with higher binding energies (858.0 and 860.4 eV, about 10%) which cannot be assigned to the above-noted nickel compounds. These may be electronic satellites [19]. Thus, an XPES study shows that the MCC-Ni nanocomposites prepared by reduction of Ni^{2+} ions in a cellulose matrix have a variable content of nanoparticles of Ni(0) and nickel oxides on the surface of MCC fibes.

The distribution of nanoparticles of Ni(0) and nickel oxides on the surface of MCC-Ni samples is shown in the electron micrographs of MCC-Ni sample nos. 1 and 2 (Figs. 4a, 4b) and in the histograms of the nickel particle-size distribution (Figs. 4c, 4d). In most cases, nanoparticles of Ni(0) and its oxides have a globular shape and are nonuniformly distributed on the surface. In some cases, nanoparticles form giant agglomerates (however, few in number). The majority of nanoparticles in sample no. 1 (>55%) have a size within 160–280 nm (Fig. 4c). Contrary to sample no. 1, the majority (about 80%) of nanoparticles in sample no. 2 have a size of about 60 nm (Fig. 4d). Sample nos. 1 and 2 were prepared at the same MR, but the diffusion of Ni^{2+} into the MCC matrix was performed at 20 and 70°C, respectively. These results show that an increase in the diffusion temperature (see table) favors formation of smaller nanoparticles of Ni and its oxides on the surface. As a rule, the size and size distribution of nanoparticles are the decisive factors governing the applicability of materials containing nanoparticles. The results of reduction of Ni^{2+} in a cellulose matrix with $N_2H_4 \cdot 2HCl$ show that nanoparticles of Ni(0) and its oxides on the surface have a smaller size than those obtained by reduction with other solvents, in particular, KH_2PO_2 [15], whereas the size of Ni(0) crystallites in the bulk does not depend essentially on the kind of reductant used (cf. data from [13, 14]).

Thus, by reduction of Ni^{2+} in an MCC matrix with $N_2H_4 \cdot 2HCl$ we found that the temperature of the Ni^{2+} diffusion into the matrix and the reductant concentration are the major factors affecting the formation of nanoparticles of Ni(0) and its oxides of widely varied size in the bulk and on the surface of MCC fibers.

CONCLUSIONS

(1) Powdered cellulose materials with the maximal content of intercalated nickel of 10.0 wt % were prepared by reduction of Ni^{2+} ions in a cellulose matrix with hydrazine dihydrochloride.

(2) The presence of nanoparticles of Ni(0) and its oxides in the bulk of the cellulose matrix was confirmed by XPA.

(3) The distribution of nanoparticles of Ni(0) and its oxides on the surface of microcrystalline cellulose fibers was studied by SEM, and the qualitative composition and oxidation state of nickel on the surface, by XPES.

REFERENCES

1. Tret'yakov, Yu.D., Lukashin, A.V., and Eliseev, A.A., *Usp. Khim.*, 2004, vol. 73, no. 9, pp. 974–998.
2. Davis, S.C., Klabunde, K.J., and Stephen, C., *Chem. Rev.*, 1982, vol. 82, no. 2, pp. 153–208.
3. Clair, A.K.St. and Taylor, L.T., *J. Appl. Polym. Sci.*, 1983, vol. 28, no. 7, pp. 2393–2400.
4. Mayer, A.B. and Mark, J.E., *Macromol. Sci. Pure Appl. Chem.*, 1997, vol. 34A, no. 11, p. 2151.
5. Gubin, S.P. and Kosodubskii, I.D., *Usp. Khim.*, 1983, vol. 52, no. 8, pp. 1350–1364.
6. Schulze, W. and Abe, H., *Faraday Soc. Symp.*, 1980, no. 14, pp. 87–93.
7. Petrov, Yu.I., *Fizika malykh chastits* (Physics of Small Particles), Moscow: Nauka. 1982.
8. Gubin, S.P., *Zh. Vseross. Khim. O–va. im. D.I. Mendeleeva*, 2000, vol. 44, no. 6, pp. 23–31.
9. Ershov, B.G., *Ross. Khim. Zh.*, 2001, vol. 45, no. 3, pp. 20–30.
10. Kotel'nikova, N.E., Wegener, G., Paakkari, T., et al., *Zh. Obshch. Khim.*, 2003, vol. 73, no. 3, pp. 447–464.
11. Kotelnikova, N.E., Paakkari, T., Serimaa, R., et al., *Macromol. Symp.*, 1999, vol. 138, pp. 175–180.
12. Kotelnikova, N.E., Kotelnikov, V.P., Nikonorova, N.I., and Serimaa, R., Abstracts of Papers, *Int. Symp. "Nanochemistry: New Approaches to Creation of Polymeric Systems with Specific Properties,"* Tashkent, 2003, p. 36.
13. Ishiyama, J.-I., Shirakawa, T., Kurokawa, Y., and Imaizumi, S., *Angew. Makromol. Chem.*, 1988, vol. 156, no. 2548, pp. 179–185.
14. He, J., Kunitake, T., and Nakao, A., *Chem. Mater.*, 2003, no. 15, pp. 4401–4406.
15. Lysenko, E.L., Kotel'nikova, N.E., and Novoselov, N.P., in *Sbornik trudov aspirantov SPGUTiD* (Coll. of Papers by Postgraduate Students of the St. Petersburg State Univ. of Technology and Design), St. Petersburg: Sankt-Peterb. Gos. Univ. Tekhnologii i Dizaina, 2005, no. 10, pp. 182–187.
16. Korovin, N.V., *Gidrazin* (Hydrazine), Moscow: Khimiya, 1980.
17. Alekseev, V.N., *Kurs kachestvennogo khimicheskogo polumikroanaliza* (Course of Qualitative Chemical Semimicroanalysis), Moscow: Khimiya, 1973.
18. *Khimicheskaya entsiklopediya* (Chemical Encyclopedia), Knunyants, I.L., Ed., Moscow: Sov. Entsiklopediya, 1961, vol. 5, pp. 455–466.
19. Moulder, J.F., Stickle, W.F., Sobol, P.E., and Vomben, K.D., *Handbook of X-ray Photoelectron Spectroscopy*, Eden Prairie: Physical Electronic, 1995.